

Half-lives of rp-process waiting point nuclei

P. Sarriguren, R. Álvarez-Rodríguez, E. Moya de Guerra
*Instituto de Estructura de la Materia, Consejo Superior de Investigaciones Científicas,
Serrano 123, E-28006 Madrid, Spain*

We give results of microscopic calculations for the half-lives of various proton-rich nuclei in the mass region $A=60-90$, which are involved in the astrophysical rp-process, and which are needed as input parameters of numerical simulations in Nuclear Astrophysics. The microscopic formalism consists of a deformed QRPA approach that involves a selfconsistent quasiparticle deformed Skyrme Hartree-Fock basis and residual spin-isospin separable forces in both the particle-hole and particle-particle channels. The strength of the particle-hole residual interaction is chosen to be consistent with the Skyrme effective force and mean field basis, while that of the particle-particle is globally fixed to $\kappa = 0.07$ MeV after a judicious choice from comparison to experimental half-lives. We study and discuss the sensitivity of the half-lives to deformation and residual interactions.

PACS: 21.60.Jz; 23.40.Hc; 26.30.+k

I. INTRODUCTION

Many problems in Nuclear Astrophysics usually require the use of numerical simulations and network calculations using weak interaction rates as input parameters [1]. High quality nuclear input is a necessary condition for a high quality astrophysical model. Thus, the models for the energy generation in stars and for nucleosynthesis may depend critically on the nuclear input used.

In particular, the rapid proton capture (rp) process is of special interest [2]. It is expected to take place in explosive scenarios, such as x-ray bursts, where the necessary conditions of high densities and temperatures are met. Actually, the relevance of the nuclear rp-process network lies in its importance as the dynamical engine of the observed x-ray bursts. The rp-process is characterized by the fact that the proton capture reaction rates are orders of magnitude faster than the competing β^+ decays. When the proton capture is inhibited, the reaction flow has to wait for a relatively slow β^+ decay to continue [2]. The longer lived β^+ emitters are called waiting points. The half-lives of the waiting point nuclei determine the time scales of the flow.

Calculations of β^+ /EC half-lives have been carried out in the past at different levels of approximation. The first large scale calculations were based on the gross theory [3]. This is a statistical model that averages over the β -strength distributions in the daughter nucleus ignoring the intrinsic nuclear structure.

More recently, many efforts have been done to calculate the weak interaction rates from microscopic calculations taking into account the nuclear structure details of the individual nuclei, see for instance [4–6]. Among the microscopic methods, the proton-neutron quasiparticle random phase approximation (pnQRPA or QRPA) is one of the most reliable and widely used microscopic approximations for calculating the correlated wave functions involved in β decay processes. The method was first studied in Ref. [7] to describe the β strength distributions. The inclusion of a particle-particle (pp) residual interaction [8], in addition to the particle-hole (ph) usual channel, and the extension of the method to deal with deformed nuclei [9–11] using phenomenological potentials, were major steps to improve the method.

Selfconsistent methods have been also applied to the study of the decay properties of spherical neutron-rich nuclei [12] and deformed proton-rich nuclei [13–15]. In the latter work, β -decay properties were studied on the basis of a deformed HF+BCS+QRPA calculation with density dependent effective interactions of Skyrme type. This is indeed a very suitable method to study the β -decay half-lives of the exotic proton-rich waiting point nuclei involved in the rp-process, namely the $N = Z$ nuclei ^{64}Ge , ^{68}Se , ^{72}Kr , ^{76}Sr , ^{80}Zr , ^{84}Mo , ^{88}Ru , and ^{92}Pd . The experimental information on half-lives existing on these nuclei is used to test the model results and to asses the predictive power of the method for network calculations of the rp-process.

The deformed HF+BCS+QRPA with density-dependent Skyrme forces and residual interactions consistent with the mean field is a method that has been successfully used in the description of the nuclear structure properties of nuclei within the valley of stability. The quality of the two-body effective Skyrme interaction and the selfconsistent procedure will finally determine the extrapolability to unknown exotic regions. Nuclear deformation is a relevant ingredient in this mass region [16], which is crossed by the rp-path, and should be included in a reliable calculation. The procedure determines the deformation selfconsistently, which is again a clear advantage in regions where there

is no experimental information on nuclear shapes. Following this method, we study in this work the half-lives of the above mentioned waiting points and their dependence on deformation and residual forces.

The paper is organized as follows. In Section 2, we present a brief summary containing the basic points in our theoretical description. Section 3 contains the results obtained for the ground state properties of the $N = Z$ waiting point nuclei considered, as well as the half-lives and their dependence on deformation and residual forces. The conclusions are given in Section 4.

II. BRIEF SUMMARY OF THE THEORETICAL FORMALISM

In this Section we summarize briefly the theoretical formalism used to describe the Gamow-Teller transitions. More details can be found in Ref. [13–15].

We follow a selfconsistent Hartree-Fock procedure to generate microscopically the deformed mean field, which is assumed to be axially symmetric. This is done with density dependent effective interactions of Skyrme type. The equilibrium deformation of the nucleus is obtained selfconsistently as the shape that minimizes the energy of the nucleus. In this work we present results obtained with the most traditional of the Skyrme forces (Sk3) [17] and with the force SG2 [18], which is known to provide a good description of the spin-isospin excitations in nuclei.

The single-particle wave functions are expanded in terms of the eigenstates of an axially symmetric harmonic oscillator in cylindrical coordinates, using eleven major shells in the expansion. Pairing correlations between like nucleons are included in the BCS approximation with fixed gap parameters for protons and neutrons. The gap parameters are determined phenomenologically from the odd-even mass differences.

Following Bertsch and Tsai [19], the particle-hole interaction consistent with the Hartree-Fock mean field is obtained as the second derivative of the energy density functional with respect to the one-body density. Neglecting momentum dependent terms, the resulting local interaction can be written in the Landau-Migdal form. After functional differentiation, one can establish a relationship between the Landau and the Skyrme parameters. The resulting residual local force is now approximated [13] by a separable force by averaging the local force over the nuclear volume assuming a constant density distribution inside a sphere with the nuclear radius. Integrating over this volume, we arrive to a separable spin-isospin force whose coupling strength is determined by the Skyrme parameters and the equilibrium radius. Hence, it varies in accordance with the Skyrme force used. The reliability of this procedure was discussed in Refs. [20,21] in the context of the spin magnetic dipole excitations, which are the $\Delta T_z = 0$ isospin counterparts of the $\Delta T_z = \pm 1$ GT transitions. The conclusion was that, although less realistic, the separable interaction contains the essential features of the zero-range force [21]. In summary, the method is a compromise between exact consistency and manageability of the residual force, which is a separable residual interaction whose strength is consistent with the ground state mean field. This procedure can be viewed as an approximation to the more general method [22], where the exact ph residual interaction is first reduced to its Landau-Migdal form and then the RPA matrix is expanded into a finite sum of n separable terms. One may expect that for radial independent RPA modes, which are considered here, the approximation made here gives a good average of the above mentioned expansion. The results in Ref. [21] support this view.

The particle-particle part is a neutron-proton pairing force in the $J^\pi = 1^+$ coupling channel. We introduce this interaction in terms of a separable force with a coupling strength, κ_{GT}^{pp} , determined by fitting the β -decay half-lives of β emitters at their equilibrium shapes.

The basic quantities needed to calculate the β -decay properties are the matrix elements connecting proton and neutron states with Fermi or Gamow-Teller operators.

We introduce the proton-neutron QRPA phonon operator for GT excitations in even-even nuclei

$$\Gamma_{\omega_K}^+ = \sum_{\pi\nu} [X_{\pi\nu}^{\omega_K} \alpha_\nu^+ \alpha_\pi^+ + Y_{\pi\nu}^{\omega_K} \alpha_\nu \alpha_\pi] , \quad (2.1)$$

where α^+ (α) are quasiparticle creation (annihilation) operators, ω_K are the RPA excitation energies, and $X_{\pi\nu}^{\omega_K}, Y_{\pi\nu}^{\omega_K}$ the forward and backward amplitudes, respectively.

In the intrinsic frame the GT transition amplitudes connecting the QRPA ground state $|0\rangle$ to one phonon states $|\omega_K\rangle$ satisfying

$$\Gamma_{\omega_K} |0\rangle = 0, \quad \Gamma_{\omega_K}^+ |0\rangle = |\omega_K\rangle , \quad (2.2)$$

are given by

$$\langle \omega_K | \sigma_K t^\pm | 0 \rangle = \mp M_\pm^{\omega_K} , \quad (2.3)$$

where

$$\begin{aligned} M_-^{\omega_K} &= \sum_{\pi\nu} (q_{\pi\nu} X_{\pi\nu}^{\omega_K} + \tilde{q}_{\pi\nu} Y_{\pi\nu}^{\omega_K}), \\ M_+^{\omega_K} &= \sum_{\pi\nu} (\tilde{q}_{\pi\nu} X_{\pi\nu}^{\omega_K} + q_{\pi\nu} Y_{\pi\nu}^{\omega_K}), \end{aligned} \quad (2.4)$$

and

$$\tilde{q}_{\pi\nu} = u_\nu v_\pi \Sigma_K^{\nu\pi}, \quad q_{\pi\nu} = v_\nu u_\pi \Sigma_K^{\nu\pi}, \quad (2.5)$$

$$\Sigma_K^{\nu\pi} = \langle \nu | \sigma_K | \pi \rangle, \quad (2.6)$$

where v 's are occupation amplitudes ($u^2 = 1 - v^2$).

The GT strength $B(GT^\pm)$ in the laboratory system for a transition $I_i K_i(0^+0) \rightarrow I_f K_f(1^+K)$ can be obtained as

$$B(GT^\pm) = \left[\delta_{K,0} \langle \omega_K | \sigma_0 t^\pm | 0 \rangle^2 + 2\delta_{K,1} \langle \omega_K | \sigma_1 t^\pm | 0 \rangle^2 \right] \quad (2.7)$$

in $[g_A^2/4\pi]$ units. We have used the initial and final states in the laboratory frame expressed in terms of the intrinsic states using the Bohr-Mottelson factorization [23]. The effect of angular momentum projection is then, to a large extent, taken into account. In the deformed cases, the spurious contributions to the strengths coming from higher angular momentum components in the wave functions are of the order $\langle J_\perp^2 \rangle^{-2}$ [24], where $\langle J_\perp^2 \rangle$ is the ground state expectation value of the angular momentum operator component perpendicular to the symmetry axis. Values of $\langle J_\perp^2 \rangle$ for the deformed nuclei considered in this work are always much larger than 10 [13] and therefore, spurious contributions are expected to represent less than 1% effect.

Similarly, the Fermi strength is obtained as

$$B(F^\pm) = |\langle \omega | t^\pm | 0 \rangle|^2, \quad (2.8)$$

in $[g_V^2/4\pi]$ units.

The β -decay half-life is obtained by summing up all the allowed transition probabilities weighted with some phase space factors up to states in the daughter nucleus with excitation energies lying within the Q -window,

$$\begin{aligned} T_{1/2}^{-1} &= \frac{1}{D} \sum_{\omega} f(Z, \omega) B_{\omega}, \\ B_{\omega} &= B_{\omega}(F) + A^2 B_{\omega}(GT), \end{aligned} \quad (2.9)$$

where $f(Z, \omega)$ is the Fermi integral [25] and $D = 6200$ s. We include standard effective factors

$$A^2 = [(g_A/g_V)_{\text{eff}}]^2 = [0.75 (g_A/g_V)_{\text{free}}]^2. \quad (2.10)$$

In β^+/EC decay, the Fermi function consists of two parts, positron emission and electron capture. In this work we have computed them numerically for each value of the energy, as explained in Ref. [25].

Although the β^+/EC half-lives are dominated by GT transitions, Fermi transitions and especially superallowed transitions to the isobaric analog state become important for nuclei with $Z > N$. We have calculated these contributions and have found that they contribute to a few percent reduction effect on the half-lives. This effect is included in the numerical results.

III. RESULTS FOR HALF-LIVES

In this Section we present first the results for the bulk properties of the nuclei under study based on the quasiparticle mean field description. We study first the energy surfaces as a function of deformation. For this purpose we perform constrained calculations [26], minimizing the HF energy under the constraint of keeping fixed the nuclear deformation. We can see in Fig. 1 the total HF energy plotted versus the quadrupole deformation parameter

$$\beta = \sqrt{\frac{\pi}{5}} \frac{Q_p}{Z r_c^2}, \quad (3.1)$$

defined in terms of the microscopically calculated quadrupole moment Q_p and charge root mean square radius r_c .

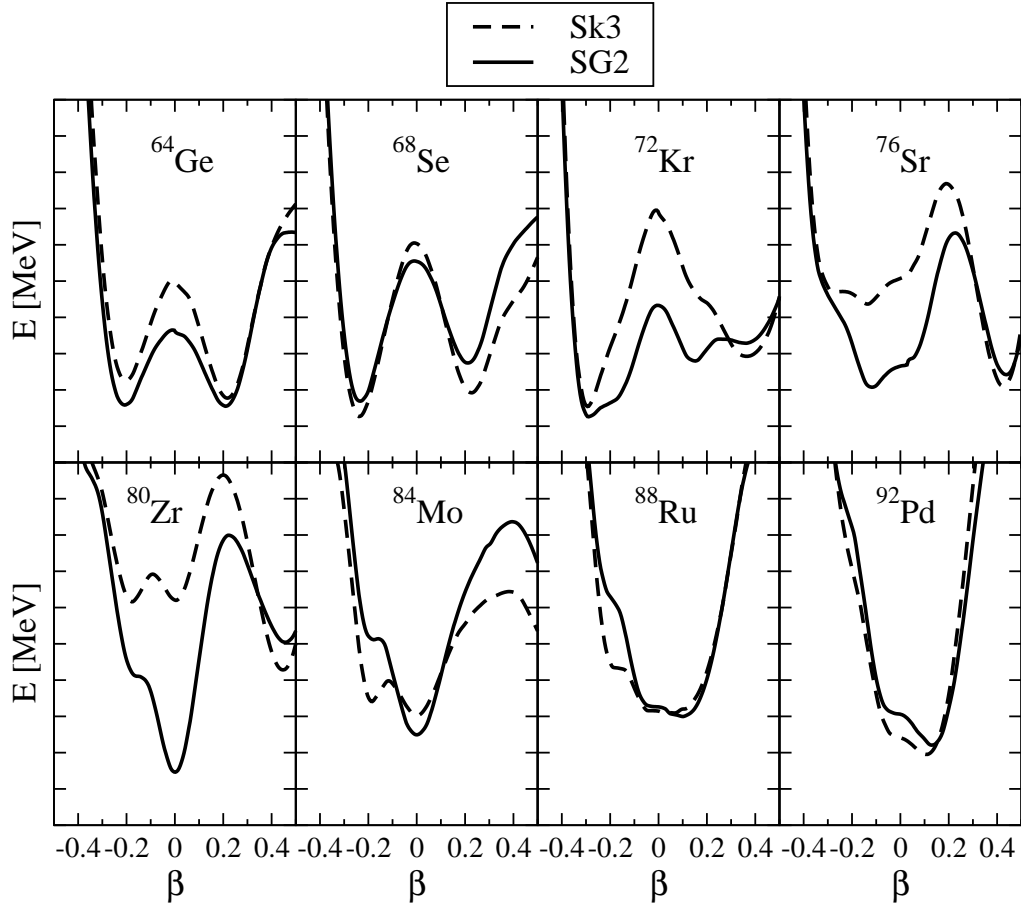


FIG. 1. Total energy as a function of the quadrupole deformation β , obtained from constrained HF+BCS calculations with various Skyrme forces. The distance between ticks in the vertical axis is always 1 MeV, but the origin is different in each case.

The results in Fig. 1 correspond to HF+BCS calculations with the forces Sk3 and SG2. We observe that both forces predict in most cases quite similar equilibrium shapes and structure of the energy curves. In some instances (^{64}Ge , ^{68}Se , ^{72}Kr , ^{76}Sr and ^{80}Zr) we obtain two energy minima close in energy, indicating the existence of shape isomers in these nuclei.

TABLE I. Charge root mean square radii r_c [fm] and quadrupole deformations β obtained with the forces Sk3 and SG2 compared with various works.

		^{64}Ge	^{68}Se	^{72}Kr	^{76}Sr	^{80}Zr	^{84}Mo	^{88}Ru	^{92}Pd
r_c	this work Sk3	4.034	4.127	4.216	4.344	4.406	4.343	4.397	4.458
	this work SG2	3.998	4.097	4.172	4.301	4.371	4.307	4.359	4.414
	Ref. [27]	3.985	4.089	4.180	4.283	4.350	4.333	4.370	4.410
β	this work Sk3	0.199	-0.216	-0.268	0.408	0.431	0.005	0.019	0.111
	this work SG2	-0.192	-0.219	-0.246	0.416	0.002	0.001	0.038	0.103
	Ref. [27]	0.217	-0.285	-0.358	0.410	0.437	-0.247	0.107	0.112
	Ref. [16]	0.219	0.240	-0.349	0.421	0.433	0.053	0.053	0.053

We can see in Table 1 the microscopically calculated charge root mean square radii r_c and quadrupole deformations as defined in Eq. (3.1). Other bulk properties, such as Q_{EC} values, of nuclei in this mass region obtained within this formalism have been already published [14], and they are in a very reasonable agreement with experiment. In this work we use the experimental Q_{EC} values [28] in the calculations of the half-lives. Since the experimental information on these nuclei is still very little, we compare in Table 1 our results with the results from relativistic mean field calculations of Ref. [27] and with results from systematic calculations [16] based on macroscopic-microscopic models (finite range droplet macroscopic model and folded Yukawa single particle microscopic model). The charge radii are quite similar but in most cases the results from SG2 are closer to the relativistic results than those calculated with Sk3. The quadrupole deformations in Table 1 correspond to the absolute minima of the energy surfaces. However, we obtain in many cases a second minimum that in some instances are very close in energy to the absolute one, as it can be seen in Fig. 1. In general we observe a good agreement among the various theoretical calculations and in those cases where a disagreement is found, the second minimum mentioned above provides the explanation. This is the case for example in ^{64}Ge , where the oblate solution in SG2 ($\beta = -0.192$) is accompanied with a prolate solution ($\beta \sim 0.2$) very close in energy (see Fig. 1). This is also the case of the spherical solution obtained for ^{80}Zr with SG2. For ^{80}Zr with SG2 we also have a prolate minimum at higher energy. This prolate shape is in agreement with the ground state solution of Sk3 and with the results from Refs. [16,27]. The case of ^{80}Zr has also been studied in Ref. [29], where the predictions of various Skyrme forces were explored. It was shown that most of these forces predict a prolate ground state with a deformation compatible with the experimental value ($\beta = 0.39$) [30], extracted by relating the measured energy of the first 2^+ excited state with the quadrupole deformation.

The results for GT strength distributions obtained from this formalism have been already tested against the experimental information available. This comparison has been done [31] in the iron mass region, where charge exchange reactions (np) and (pn) have been measured, and $B(GT^+)$ and $B(GT^-)$ have been extracted. The agreement with experiment is very good and comparable to the results obtained from full shell model calculations [32]. Results for odd-A nuclei have been analyzed and compared to experiment in Ref. [15] on the example of Kr isotopes. The method has also been used to analyze the recently measured [33] GT strength distributions in ^{74}Kr and ^{76}Sr . The dependence on deformation of these distributions allows one to conclude that the decay pattern of ^{76}Sr is compatible with a prolate shape while that of ^{74}Kr requires an admixture of oblate and prolate shapes.

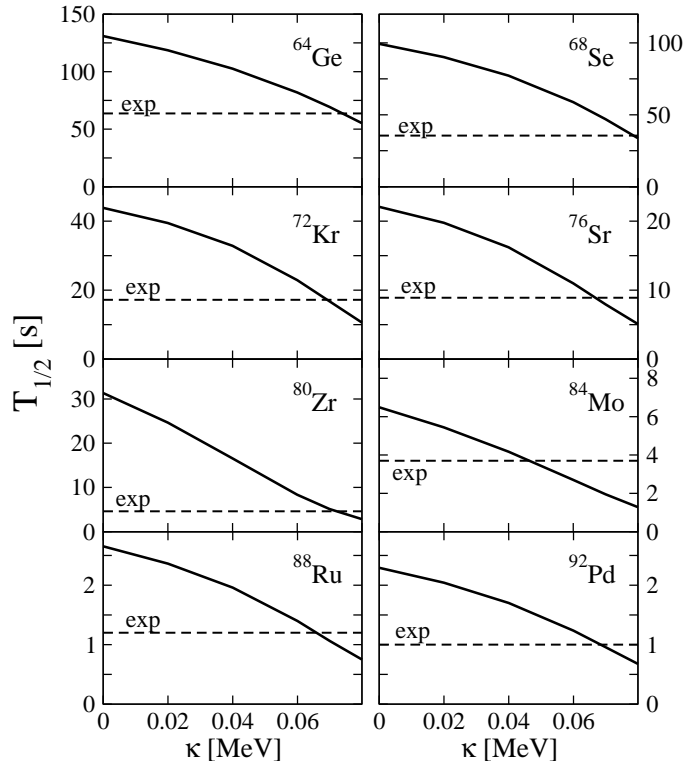


FIG. 2. Half-lives of the $N = Z$ waiting points ($A=64-92$) obtained with the force SG2 as a function of the pp coupling strength κ compared to experiment (dashed lines).

Once the reliability of the method has been contrasted, we proceed now with the calculation of the half-lives in the waiting point nuclei. Fig. 2 shows the dependence of $T_{1/2}$ on the strength of the pp residual interaction, using the Skyrme force SG2. As we have mentioned, the ph strength is fixed by the Skyrme force in a consistent way but the pp strength remains undetermined. The half-lives for all the waiting points in this region are plotted in Fig. 2 as a function of κ_{GT}^{pp} for the equilibrium deformations that minimize the energy (see Table 1). As we increase κ_{GT}^{pp} , the GT strength is reduced and shifted to lower energies. Below the Q_{EC} window there is a competition between the global reduction of the GT strength and the accumulation of extra strength at lower energies. The latter effect becomes dominant and the half-lives are suppressed as we increase κ_{GT}^{pp} . The experimental half-life is reproduced in almost all cases with values of κ_{GT}^{pp} around 0.07 and therefore this is the value postulated to be used in those cases where the half-lives have not been measured yet.

In Fig.3 we study the sensitivity of $T_{1/2}$ to deformation. We use the force SG2 and $\kappa_{GT}^{pp} = 0.07$ MeV. We can see how the HF+BCS half-lives are systematically lower than the QRPA and experiment, sometimes even by one order of magnitude. QRPA correlations reduce the mean field GT strength and as a result the half-lives increase accordingly. Deformation can also change the half-lives by factors up to four. What is remarkable is that the experimental half-lives are systematically better reproduced for the selfconsistent deformations that minimize the energy, as can be seen by comparing Fig. 3 with the SG2 minima in Fig. 1. The same feature is found with the Sk3 force. This shows to what extent selfconsistency plays an important role in the calculation of the half-lives. In this respect, it is interesting to note that with the SG2 force, the experimental value of $T_{1/2}$ for ^{80}Zr is reproduced at the SG2 equilibrium deformation ($\beta \sim 0$), but not at the experimental deformation ($\beta \sim 0.4$) that corresponds to a higher local minimum.

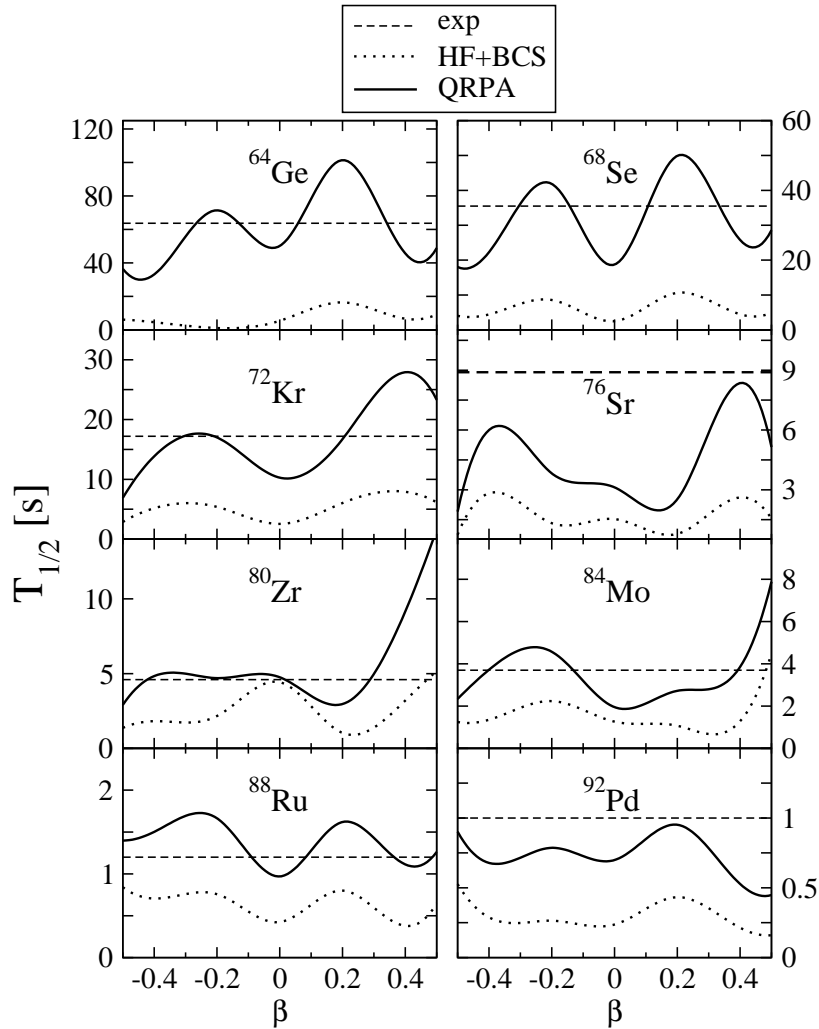


FIG. 3. Dependence of the half-life with deformation, using the force SG2. The results correspond to HF+BCS (dotted) and QRPA (solid) calculations with $\kappa_{GT}^{pp} = 0.07$ MeV. Experimental values are shown by dashed lines.

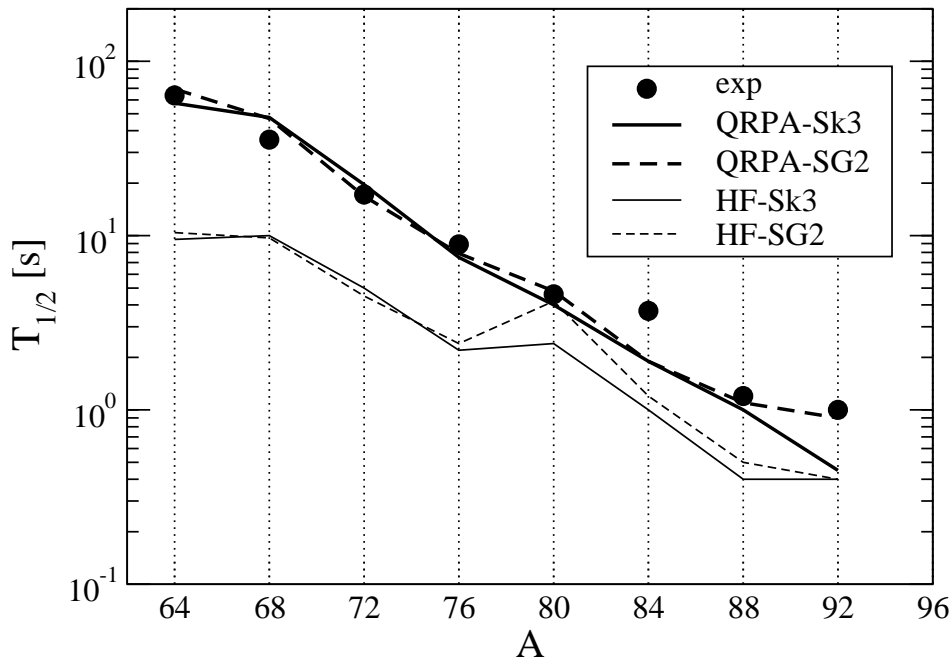


FIG. 4. Half-lives of the $N = Z$ waiting points ($A=64-92$) obtained within various approaches and compared to experiment [28] for $A=64,68,72,76,80$ and [34] for $A=84,88,92$.

Finally in Fig. 4 we show the results for the half-lives obtained from our approach in the even-even $N = Z$ waiting points from $A=64$ up to $A=92$. The results correspond to the forces Sk3 and SG2 with the deformations and coupling strengths residual forces discussed above. Again, the HF+BCS results appear systematically below the QRPA results and below the experiment. The QRPA results from both forces agree nicely with experiment. We get also in general agreement with the QRPA results obtained from a different formalism based on Yukawa potentials [4].

IV. CONCLUSIONS

Using a deformed QRPA formalism, based on a selfconsistent quasiparticle mean field, which includes ph and pp separable residual interactions, we have studied the β -decay properties of several $N = Z$ waiting point nuclei involved in the astrophysical rp-process.

We have analyzed the half-lives as a function of deformation and residual interactions and have found that best agreement with the laboratory experimental half-lives is obtained using: a) the selfconsistent deformations obtained from the minimization of the energy, and b) residual interactions with a consistently derived ph strength and $\kappa_{GT}^{pp} = 0.07$ MeV.

The results obtained indicate that this formalism is a useful method for reliable calculations of half-lives. This is especially interesting for applications to: i) cases where no experimental information is available; ii) nuclei under different conditions of densities and temperatures; and iii) nuclei that are beyond the capability of full shell model calculations. Work under these lines is in progress.

Acknowledgments

This work was supported by Ministerio de Educación y Ciencia (Spain) under contract number BFM2002-03562. One of us (R.A.-R.) thanks Ministerio de Educación y Ciencia (Spain) for financial support.

- [1] K. Grotz and H.V. Klapdor, *The Weak Interaction in Nuclear, Particle and Astrophysics*, (IOP, Bristol, 1990); K. Langanke and G. Martínez-Pinedo, *Rev. Mod. Phys.* **75**, 819 (2003).
- [2] H. Schatz *et al.*, *Phys. Rep.* **294**, 167 (1998).
- [3] K. Takahashi, M. Yamada, T. Kondoh, *At. Data Nucl. Data Tables* **12**, 101 (1973); T. Kondoh, T. Tachibana and M. Yamada, *Prog. Theor. Phys.* **74**, 708 (1985).
- [4] P. Moeller, J.R. Nix and K.-L. Kratz, *At. Data Nucl. Data Tables* **66**, 131 (1997).
- [5] J.-U. Nabi and H.V. Klapdor-Kleingrothaus, *At. Data Nucl. Data Tables* **71**, 149 (1999).
- [6] K. Langanke and G. Martínez-Pinedo, *Nucl. Phys. A* **673**, 481 (2000); *At. Data Nucl. Data Tables* **79**, 1 (2001).
- [7] J.A. Halbleib and R.A. Sorensen, *Nucl. Phys. A* **98**, 542 (1967).
- [8] P. Vogel and M.R. Zirnbauer, *Phys. Rev. Lett.* **57**, 3148 (1986); D. Cha, *Phys. Rev. C* **27**, 2269 (1987).
- [9] J. Krumlinde and P. Moeller, *Nucl. Phys. A* **417**, 419 (1984).
- [10] P. Moeller and J. Randrup, *Nucl. Phys. A* **514**, 1 (1990).
- [11] H. Homma, E. Bender, M. Hirsch, K. Muto, H.V. Klapdor-Kleingrothaus and T. Oda, *Phys. Rev. C* **54**, 2972 (1996).
- [12] J. Engel, M. Bender, J. Dobaczewski, W. Nazarewicz, and R. Surnam, *Phys. Rev. C* **60**, 014302 (1999); M. Bender, J. Dobaczewski, J. Engel, and W. Nazarewicz, *Phys. Rev. C* **65**, 054322 (2002).
- [13] P. Sarriguren, E. Moya de Guerra, A. Escuderos, and A.C. Carrizo, *Nucl. Phys. A* **635**, 55 (1998); P. Sarriguren, E. Moya de Guerra, and A. Escuderos, *Nucl. Phys. A* **658**, 13 (1999).
- [14] P. Sarriguren, E. Moya de Guerra, and A. Escuderos, *Nucl. Phys. A* **691**, 631 (2001).
- [15] P. Sarriguren, E. Moya de Guerra, and A. Escuderos, *Phys. Rev. C* **64**, 064306 (2001).
- [16] P. Moeller, J.R. Nix, W.D. Myers, W.J. Swiatecki, *At. Data Nucl. Data Tables* **59**, 185 (1995).
- [17] M. Beiner, H. Flocard, N. Van Giai, and P. Quentin, *Nucl. Phys. A* **238**, 29 (1975).
- [18] N. Van Giai and H. Sagawa, *Phys. Lett. B* **106**, 379 (1981).
- [19] G.F. Bertsch and S.F. Tsai, *Phys. Rep.* **18**, 127 (1975).
- [20] P. Sarriguren, E. Moya de Guerra and R. Nojarov, *Phys. Rev. C* **54**, 690 (1996); *Z. Phys. A* **357**, 143 (1997).
- [21] D. Zawisha and J. Speth, *Nucl. Phys. A* **569**, 343c (1994).
- [22] N. Van Giai, Ch. Stoyanov and V.V. Voronov, *Phys. Rev. C* **57**, 1204 (1998); A.P. Severyukhin, Ch. Stoyanov, V.V. Voronov and N. Van Giai, *Phys. Rev. C* **66**, 034304 (2002).
- [23] A. Bohr and B. Mottelson, *Nuclear Structure* (Benjamin, New York 1975).
- [24] E. Moya de Guerra, *Phys. Rep.* **138**, 293 (1986).
- [25] N.B. Gove and M.J. Martin, *Nucl. Data Tables* **10**, 205 (1971).
- [26] H. Flocard, P. Quentin, A.K. Kerman, and D. Vautherin, *Nucl. Phys. A* **203**, 433 (1973).
- [27] G.A. Lalazissis, S. Raman and P. Ring, *At. Data Nucl. Data Tables* **71**, 1 (1999).
- [28] G. Audi, O. Bersillon, J. Blachot and A.H. Wapstra, *Nucl. Phys. A* **729**, 3 (2003).
- [29] P.-G. Reinhard, D.J. Dean, W. Nazarewicz, J. Dobaczewski, J.A. Maruhn and M.R. Strayer, *Phys. Rev. C* **60**, 014316 (1999).
- [30] C.J. Lister, M. Campbell, A.A. Chishti, W. Gelletly, L. Goettig, R. Moscrop, B.J. Varley, A.N. James, T. Morrison, H.G. Price, J. Simpson, K. Connel and O. Skeppstedt, *Phys. Rev. Lett.* **59**, 1270 (1987).
- [31] P. Sarriguren, E. Moya de Guerra and R. Álvarez-Rodríguez, *Nucl. Phys. A* **716**, 230 (2003).
- [32] E. Caurier, K. Langanke, G. Martínez-Pinedo and F. Nowaki, *Nucl. Phys. A* **653**, 439 (1999).
- [33] E. Poirier *et al.*, *Phys. Rev. C* **69**, 034307 (2004); E. Náchter *et al.*, *Phys. Rev. Lett.* **92**, 232501 (2004).
- [34] P. Kienle *et al.*, *Prog. Part. Nucl. Phys.* **46**, 73 (2001).